

Spatial extension as a “smoking gun” for dark subhalo detection with *Fermi*-LAT and implications for WIMP constraints

Javier Coronado-Blázquez, ^{a,b,*} Miguel A. Sánchez-Conde, ^{a,b} Judit Pérez-Romero, ^{a,b} Alejandra Aguirre-Santaella, ^{a,b} on behalf of the *Fermi*-LAT Collaboration

^a*Instituto de Física Teórica IFT UAM-CSIC,
C/Nicolás Cabrera 13-15, Madrid, Spain*

^b*Departamento de Física Teórica, Universidad Autónoma de Madrid,
Campus de Cantoblanco, Madrid, Spain
E-mail: javier.coronado@uam.es, miguel.sanchezconde@uam.es,
judit.perez@uam.es, alejandra.aguirre@uam.es*

Spatial extension has been hailed as a “smoking gun” in the gamma-ray search of dark galactic subhalos, which would appear as unidentified sources for gamma-ray telescopes. In this work, we study the actual sensitivity of the *Fermi*-LAT to extended subhalos using simulated data based on a realistic sky model for the first time. We generate spatial templates for a set of representative subhalos, whose parameters were derived from our previous work with N-body cosmological simulation data. We find that detecting an extended subhalo and finding an unequivocal signal of angular extension requires, respectively, a flux 2 to 10 times larger than in the case of a point-like source. By studying a large grid of models, where parameters such as the WIMP mass, annihilation channel or subhalo model are varied significantly, we obtain the response of the LAT as a function of the product of annihilation cross section times the J-factor. Indeed, we show that spatial extension can be used as an additional “filter” to reject subhalos candidates among the pool of unidentified LAT sources, as well as a “smoking gun” for positive identification. We conclude that typical angular extensions of about 0.3° are expected for the considered scenarios. Finally, we also study the impact of the obtained LAT sensitivity to such extended subhalos on the achievable dark matter constraints, that now worsen by a factor of a few with respect to the point-source limits.

37th International Cosmic Ray Conference (ICRC 2021)
July 12th – 23rd, 2021
Online – Berlin, Germany

*Presenter

1. Introduction

The nature of dark matter (DM), a non-baryonic component of the Universe accounting up to $\sim 25\%$ of its matter-energy density, is one of the most pressing questions in modern physics. In the case of indirect DM detection, looking for the annihilation (or decay) products of DM, gamma rays have been considered a “golden channel”, as they are not deflected by magnetic fields (as opposed to antimatter produced in DM annihilation or decays), and are easier to detect than neutrinos. With gamma-ray telescopes, many different targets have been observed, such as the Galactic center (GC), dwarf spheroidal galaxies (dSphs) and galaxy clusters [1].

An interesting and complementary target for gamma-ray searches are the so-called dark subhalos (also known as dark satellites). Within the standard Λ -Cold Dark Matter (Λ CDM) cosmological paradigm, the DM halos that host galaxies should contain a large amount of substructure (subhalos, i.e., halos within halos) as a consequence of the bottom-up hierarchical structure formation scenario. The largest members of this subhalo population (above $\sim 10^7 M_\odot$) will host dSphs, yet most of them are not massive enough to retain baryonic content, i.e., gas, and form stars, and therefore should remain completely dark [2]. If near enough and composed of WIMPs, they would yield a significant flux of gamma rays that could be detected by gamma-ray telescopes such as the *Fermi*-Large Area Telescope (LAT) on board the NASA *Fermi* satellite [3].

A large number of *Fermi*-LAT sources lack clear astrophysical association and have no multi-wavelength counterparts, remaining as unidentified sources (unIDs) at present. These are perfect candidates to perform a search for Galactic dark subhalos, as WIMPs may be annihilating within them, appearing as unIDs in the LAT sky. In previous works, [4, 5] we applied a series of filters to the unIDs according to the expected emission from dark subhalo annihilation, and performed a dedicated spectral analysis to enforce or reject the DM hypothesis. Only a handful of them showed some preference to a DM origin over a traditional astrophysical explanation, yet at a small statistical significance.

In [5], source spatial extension was pointed out to be a “smoking gun” for this kind of indirect DM searches. Indeed, in [5] we quantified for the first time the expected extension of the brightest (i.e., easiest to detect) subhalos, as obtained from our repopulated N-body simulations. Very large angular sizes, $O(5^\circ)$ were found when integrating the annihilation signal up to the scale radius. In this work, we convolute the predicted signal with the instrumental sensitivity of the LAT to obtain a reliable characterization of the LAT capabilities for extended DM subhalos.

2. Gamma-ray signal from Milky Way subhalos

In Λ CDM, we can distinguish between dSphs, which have a baryonic counterpart, and dark satellites, which do not have it. We expect most Galactic DM subhalos to be of the latter kind. In our previous works [4] and [5], we adopted a conservative upper mass limit of $M_{sub} < 10^7 M_\odot$ for these objects, thus we will stick to this bound here as well. To quantitatively measure the expected annihilation flux, we define the so-called J-factor for a subhalo as:

$$J_{sub}(\Delta\Omega, l.o.s) = \int_0^{\Delta\Omega} d\Omega \int_{l.o.s} \rho^2(r) dl, \quad (1)$$

where $\Delta\Omega = 2\pi(1 - \cos \alpha_{int})$, with α_{int} the integration angle, the integration is calculated along the line of sight (*l.o.s.*) and $\rho(r)$ is the DM density profile. Subhalos with the highest expected annihilation fluxes, i.e., at least $J_{sub} \gtrsim 10^{19} \text{ GeV}^2 \text{ cm}^{-5}$, are the most interesting for our purposes. Given the large number of subhalos above this value, as well as the large spread in their masses and distances, it becomes unfeasible to perform a *Fermi-LAT* analysis simulation for each of them. In view of this, we decided to select two representative scenarios. As already stated before, we want to restrict ourselves to dark subhalos. This implies that the highest mass we can reach would be $10^7 M_\odot$, following our previous work and results found, e.g., in [2]. We consider two models: i) a subhalo with a small mass of $M_{sub} = 10^4 M_\odot$ located near Earth ($D_{\text{Earth}} = 0.5 \text{ kpc}$); and ii) a subhalo with a mass in the limit of $M_{sub} = 10^7 M_\odot$ and situated far from Earth ($D_{\text{Earth}} = 10 \text{ kpc}$).

With this selection of representative cases, we aim at covering the range in masses, distances and expected angular extensions of the fraction of the subhalo population expected to be relevant for our purposes. The obtained profile parameters for each of the two representative subhalo scenarios are given in Table 1.

Name	D_{Earth} [kpc]	M_{sub} [M_\odot]	c_{200}	r_s [kpc]	R_{tidal} [kpc]	$\log_{10} \rho_0$ [M_\odot/kpc^3]
Subhalo 1	0.5	10^4	71.36	0.006	0.036	9.00
Subhalo 2	10	10^7	42.31	0.107	0.516	2.95

Table 1: Parameters needed to build the NFW DM profiles of our two subhalo scenarios, each of them representatives of the fraction of the Galactic dark subhalo population that is relevant in terms of expected annihilation flux.

The DM modeling performed in the previous section is the starting point for obtaining the expected DM-induced gamma-ray flux for the two representative subhalo cases. Assuming that the DM is made of Majorana WIMPs, the annihilation flux can be computed as:

$$\frac{d\phi_\gamma}{dE}(E, \Delta\Omega, l.o.s.) = \frac{1}{8\pi m_{DM}^2} \langle \sigma v \rangle \frac{dN_\gamma}{dE}(E) \times J(\Delta\Omega, l.o.s.), \quad (2)$$

where $\frac{d\phi_\gamma}{dE}$ is the differential gamma-ray flux, $\langle \sigma v \rangle$ is the velocity-averaged annihilation cross-section, m_{DM} is the DM mass, $\frac{dN_\gamma}{dE}$ is the photon spectrum and J is the astrophysical factor or J-factor defined as in Eq. 1. We notice that two main dependencies can be identified in the flux. First, an energy dependence that appears only in the particle physics term, carrying all the information of the mass of the DM candidate and the annihilation channels. Secondly, the spatial dependence appearing as the J-factor. This allows us to factorize these terms independently, and to model the spatial distribution of the DM independently of energy. The photon spectrum from DM annihilation strongly depends on the mass of the dark matter particle and on the annihilation channel, which indeed leads to very different spectra depending on which combinations are selected. We will explore the impact on the gamma-ray flux of these dependencies in Section 3.

The computation of the J-factors is performed using the CLUMPY code [6], which allows us to model the DM profiles of the subhalos as described above and to compute J-factors, annihilation fluxes, etc. The obtained values of the integrated J-factors for each considered subhalo model are shown in Table 2.

Name	$\log_{10} J_{sub}$ [GeV ² cm ⁻⁵]	$\log_{10} J_s$ [GeV ² cm ⁻⁵]
Subhalo 1	19.20	19.17
Subhalo 2	19.14	19.10

Table 2: Total, integrated J-factors for the two representative subhalo scenarios, in the first column integrated up to the whole object (R_{sub}), and up to r_s in the second.

The results shown in Table 2 show an emerging degeneracy between the two considered physical scenarios chosen as representative of the population of subhalos in the MW relevant in terms of annihilation flux. Indeed, both scenarios will be nearly indistinguishable in terms of the expected annihilation flux, despite the fact that both physical scenarios were defined independently. In order to take a closer look at this degeneracy, we can also use CLUMPY to create two-dimensional templates, reproducing the spatial morphology of the expected DM annihilation signal. These maps are shown in Figure 1 for the two representative subhalos, and represent, indeed, the main CLUMPY result that will be later used for the LAT analysis. The figure also exhibits the same degeneracy between the two scenarios that appeared before in Table 2 for the integrated J-factors.

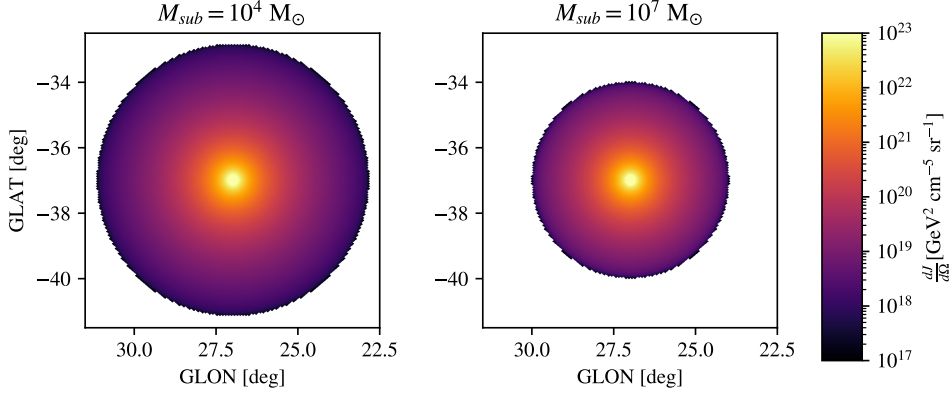


Figure 1: Two-dimensional templates of the DM-induced gamma-ray spatial morphology for the two representative subhalo scenarios. The z axis represents the differential J-factor ($\frac{dJ}{d\Omega}$) computed according to the DM modeling explained in Section 2.

3. LAT sensitivity to extended dark matter subhalos

In this section, we will compute the actual sensitivity of the LAT to an extended DM subhalo in the two subhalo mass modeling scenarios described in Section 2. For each subhalo model, we will consider two benchmark annihilation channels: $b\bar{b}$, representative of hadronic final states, and $\tau^+\tau^-$, representative of leptonic ones.

First, we compute the minimum flux that is needed in order to detect an extended subhalo with the Fermi-LAT. To do so, we simulate the LAT sensitivity by placing a putative, extended DM subhalo in the sky. Then, we vary the normalization of the source until it reaches detection – at that very moment the integrated flux will be the minimum detection flux.

To perform such computation, we rely on *fermipy* [7]. We use 11 years of LAT data, with an energy range between 500 MeV and 2 TeV, Pass 8 events, with the P8R3_SOURCE_V2 instrumental response functions (IRFs), and utilize all available photons (FRONT+BACK), excluding those arriving with zenith angles greater than 105° . The region of interest (ROI) is taken as a $15^\circ \times 15^\circ$ area. To model point sources lying within the ROI, we use the second release of the latest LAT point-source catalog, 4FGL-DR2 [8], version `gll_psc_v27.fit`. In the analysis, the `gll_iem_v07.fits` and `iso_P8R3_SOURCE_V2.txt` templates are used to model the Galactic and isotropic diffuse emission, respectively. The subhalo flux normalization is defined as,

$$\mathcal{N} = J \times \langle \sigma v \rangle \left[\text{GeV}^2 \cdot \text{cm}^{-2} \cdot \text{s}^{-1} \right], \quad (3)$$

where J is the J-factor and $\langle \sigma v \rangle$ is the velocity-averaged annihilation cross section as introduced in Eq. 1. Indeed, the spectrum normalization is completely degenerated between these two quantities, and therefore we will discuss the results based on this overall normalization from now on. To compute the detection or extension significance of the source, we adopt the Test Statistic [9],

$$\text{TS} = 2 \cdot \log \left[\frac{\mathcal{L}(H_1)}{\mathcal{L}(H_0)} \right], \quad (4)$$

where $\mathcal{L}(H_0)$ and $\mathcal{L}(H_1)$ are, respectively, the likelihoods under the null (no source/point-like) and alternative (existing DM source/extended) hypotheses. To ensure either a robust source detection or an unequivocal extended source, we will search for the minimum flux value (F_{min}) that would yield at least $\text{TS}_{\text{det}} = 25$ or $\text{TS}_{\text{ext}} = 25$, respectively.

We repeat each configuration of subhalo modeling, WIMP mass, and annihilation channel 10 times for both our evaluation of subhalo detection and detection of extension. We can also compare the detection and extension fluxes with respect to the PS case, i.e., with no spatial template. This is shown in Figure 2. In Figure 2 we show the results. There is a consistent trend of obtaining lower fluxes for larger WIMP masses in every case. Moreover, it is interesting to compare the ratios between the three of them; when analyzing detection ($\text{TS}_{\text{det}} = 25$), we can distinguish between the PS and extended cases. The latter turns out to be a factor 1.5 – 2 larger (meaning more difficult to detect), as the photons are spatially spread, and therefore the sensitivity is slightly decreased. Nevertheless, being that the DM annihilation profile is very cuspy (see Section 2), most of the signal comes from the innermost part of the profile, and there is little difference with respect to the PS case. This is no longer true for the case of detection of extension ($\text{TS}_{\text{ext}} = 25$), where the required fluxes are a factor 8 – 10 larger than in the PS case (and therefore a factor 4 – 6 larger than the F_{min}^{det} for the extended template). This trend is observed in every channel and subhalo model. As already noted in Section 2, the two considered subhalo models are completely degenerate from the point of view of detection and extension analysis.

We can also study a more general performance of the instrument in a wider range of subhalo configurations, varying the same parameters (different subhalo models, WIMP masses, annihilation channels) and including new normalization values – not searching for a specific value of detection/extension significance but rather blindly studying the output with different normalizations. To do so, we will define the grid of models to be studied. We choose an \mathcal{N} grid which will be representative of viable DM models (even if extreme in some cases), with 15 values logarithmically spaced between $\mathcal{N} = 10^{-6} - 10^{-3}$ (i.e., 5 values per order of magnitude).

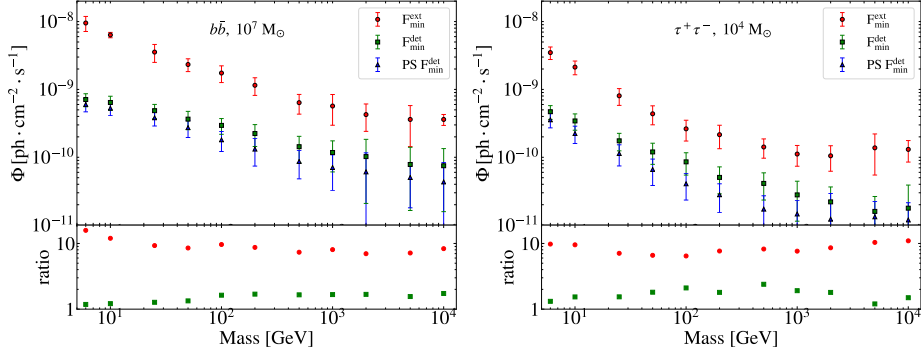


Figure 2: Minimum fluxes for point-source (PS) and extended subhalo detection (F_{min}^{det}), and extension with $\text{TS}_{ext} = 25$ (F_{min}^{ext}), for $b\bar{b}$ (left panel) and $\tau^+\tau^-$ (right panel) annihilation channels. Lower panels show the ratio between F_{min}^{det} (green squares) and F_{min}^{ext} (red circles) when compared to the PS threshold.

In Figure 3, we show the angular extension (computed as R_{68} , i.e., the region where 68% of the signal is contained) as a function of both TS_{det} and TS_{ext} . Below $\lesssim 500$ GeV, the LAT is able to recover spatial information with $\text{TS}_{ext} > 25$. Above these masses, the instrumental performance is degraded and only hints of extension can be found, yet not pointing to a point-like source.

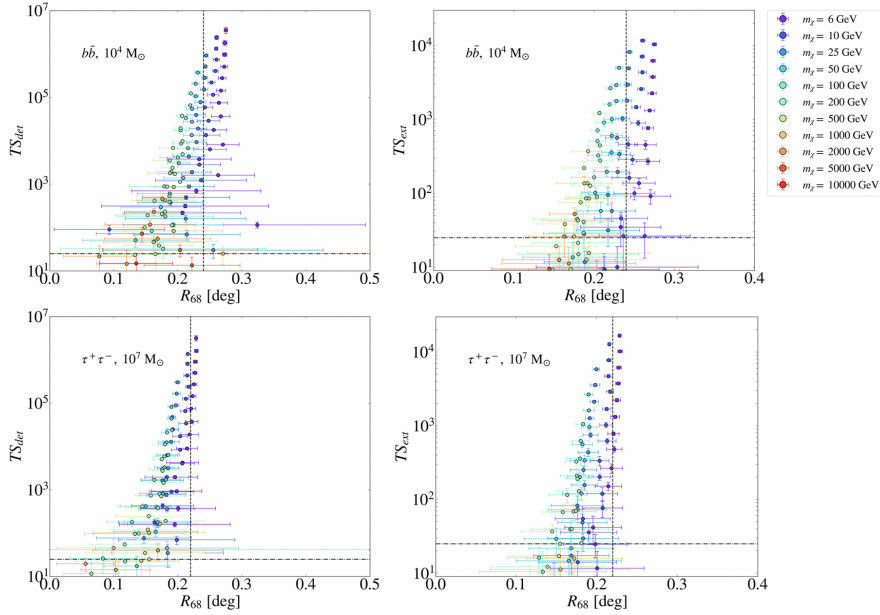


Figure 3: Best-fit extension R_{68} versus the extension (TS_{ext}) and detection (TS_{det}) significance, for the ($b\bar{b}$, $10^4 M_\odot$) and the ($\tau^+\tau^-$, $10^7 M_\odot$) models. Each R_{68} is the average value of the 10 realizations, while their uncertainties are computed via a quadratic sum of the individual realization uncertainties and the 1σ spread across realizations.

4. Implications for WIMP dark matter constraints

Our study on the characterization of the spatial extension of a potential dark subhalo signal in LAT data could have relevant implications for the case of setting DM constraints with unIDs.

Following the methodology in [4], we now compute constraints on the WIMP mass vs. annihilation cross section parameter space, yet integrating the J-factor up to 0.3° instead of the scale radius. This will effectively result in lower J-factors, which will degrade the achievable constraints. In Figure 4, we show the constraints for both the $\tau^+\tau^-$ and $b\bar{b}$ annihilation channels as a function of the number of sources (in log-scale) compatible with DM.

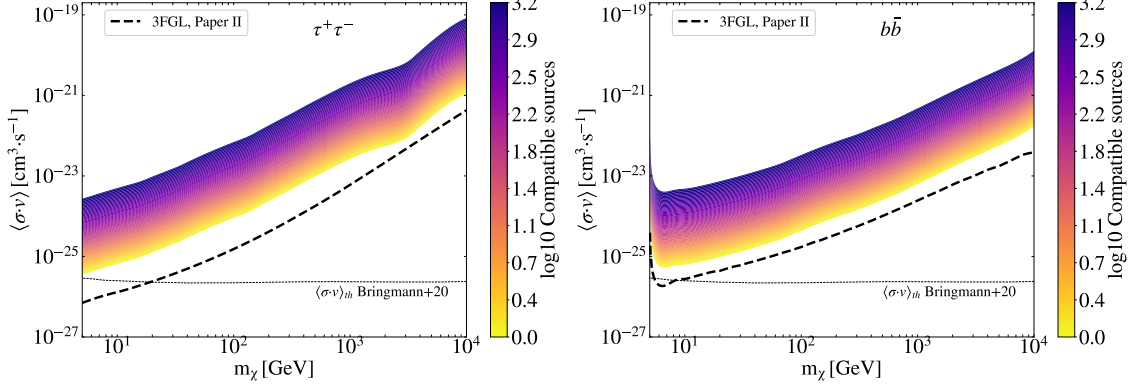


Figure 4: 95% C.L. limits for DM annihilating to $\tau^+\tau^-$ (left panel) and $b\bar{b}$ (right panel), as a function of the number of 4FGL–DR2 unIDs compatible with DM. Black, dashed line is the constraint obtained in [5] using the previous 3FGL catalog [10] with 1 (5) compatible sources in the case of $\tau^+\tau^-$ ($b\bar{b}$) channel, starting the analysis at 100 MeV, assuming point-like sources and integrating the J-factor up to the scale radius. The horizontal dashed line is the thermal relic cross section [11].

Even in the sensitivity reach case (one source), we do not achieve the constraints we set in [5] by means of the 3FGL catalog [10]. We recall that in the case of [5], the constraints for $\tau^+\tau^-$ channel were already at sensitivity reach level, which are now a factor ~ 8 away for low WIMP masses and a factor ~ 5 away for the heaviest WIMPs. Overall, in the sensitivity reach case, our new constraints are right at the thermal relic cross section value for the lowest considered WIMP masses and a factor ~ 10 away at 100 GeV in the case of $\tau^+\tau^-$ annihilation channel, while similar conclusions can be drawn for $b\bar{b}$, yet a factor ~ 4 far from the thermal value at best.

5. Conclusions

In this work, we characterized the capabilities of the *Fermi*-LAT gamma-ray telescope to observe extended DM subhalos. These would appear as unIDs in the gamma-ray sky, and can be spatially modeled with the CLUMPY software with two extreme and representative scenarios. When analysing the data with fermipy, we find the necessary flux to detect a subhalo to be a factor ~ 2 larger than the point-like case, and a factor ~ 10 larger to properly characterize the spatial signal. When studying the angular extension, we find the LAT is able to recover spatial information for light WIMPs (below $\lesssim 500$ GeV). Finally, the constraints are re-computed integrating the signal up to the innermost 0.3° , as suggested by the results. This degrades the achievable constraints a factor ~ 8 with respect to the point-like case.

Acknowledgements

The *Fermi*-LAT Collaboration acknowledges support for LAT development, operation and data analysis from NASA and DOE (United States), CEA/Irfu and IN2P3/CNRS (France), ASI and INFN (Italy), MEXT, KEK, and JAXA (Japan), and the K.A. Wallenberg Foundation, the Swedish Research Council and the National Space Board (Sweden). Science analysis support in the operations phase from INAF (Italy) and CNES (France) is also gratefully acknowledged. This work performed in part under DOE Contract DE-AC02-76SF00515.

References

- [1] J. Conrad and O. Reimer, *Indirect dark matter searches in gamma and cosmic rays*, *Nature Physics* **13** (mar, 2017) 224–231.
- [2] T. Sawala, C. S. Frenk, A. Fattahi, J. F. Navarro, T. Theuns, R. G. Bower et al., *The chosen few: the low-mass haloes that host faint galaxies*, *Monthly Notices of the Royal Astronomical Society* **456** (Dec, 2015) 85–97.
- [3] The Fermi-LAT Collaboration and W. B. Atwood, *The Large Area Telescope on the Fermi Gamma-ray Space Telescope Mission*, *APJ* (2009) , [0902.1089v1].
- [4] J. Coronado-Blázquez, M. A. Sánchez-Conde, A. Domínguez, A. Aguirre-Santaella, M. D. Mauro, N. Mirabal et al., *Unidentified gamma-ray sources as targets for indirect dark matter detection with the Fermi-Large Area Telescope*, *Journal of Cosmology and Astroparticle Physics* **2019** (jul, 2019) 020–020.
- [5] J. Coronado-Blázquez, M. A. Sánchez-Conde, M. D. Mauro, A. Aguirre-Santaella, I. Ciucă, A. Domínguez et al., *Spectral and spatial analysis of the dark matter subhalo candidates among Fermi Large Area Telescope unidentified sources*, *Journal of Cosmology and Astroparticle Physics* **2019** (nov, 2019) 045–045.
- [6] M. Hütten, C. Combet and D. Maurin, *CLUMPY v3: γ -ray and ν signals from dark matter at all scales*, *Computer Physics Communications* **235** (feb, 2019) 336–345.
- [7] M. Wood, R. Caputo, E. Charles, M. D. Mauro, J. Magill and J. Perkins, *Fermipy: An open-source Python package for analysis of Fermi-LAT Data*, 1707.09551.
- [8] J. Ballet, T. H. Burnett, S. W. Digel and B. Lott, *Fermi Large Area Telescope Fourth Source Catalog Data Release 2*, 2005.11208.
- [9] J. Rico, *Gamma-Ray Dark Matter Searches in Milky Way Satellites—A Comparative Review of Data Analysis Methods and Current Results*, *Galaxies* **8** (Mar, 2020) 25.
- [10] The Fermi-LAT Collaboration, *Fermi Large Area Telescope Third Source Catalog*, *The Astrophysical Journal Supplement Series* **218** (jun, 2015) 23.
- [11] T. Bringmann, P. F. Depta, M. Hufnagel and K. Schmidt-Hoberg, *Precise dark matter relic abundance in decoupled sectors*, 2007.03696.